www.editada.org

International Journal of Combinatorial Optimization Problems and Informatics, 16(3), May-Aug 2025, 46-63. ISSN: 2007-1558.
https://doi.org/10.61467/2007.1558.2025.v16i3.1130

Design of a Robotic Device for Arm Rehabilitation

Elihu H. Ramirez-Dominguez[1], *José G. Benítez-Morales* [1], *Ángel R. Licona-Rodríguez* [1], *Ma. de Angeles Alamilla Daniel* [1], Javier Hernández-Pérez [1], Juan Manuel Xicoténcatl-Pérez [1]
[1] Universidad Politécnica de Pachuca, Pachuca, México.
E-mails: elihuhadad@gmail.com, josegerardo@upp.edu.mx, arliconar@upp.edu.mx, alamillameca@upp.edu.mx, jahdez@upp.edu.mx, jmxico@upp.edu.mx

Abstract. This article presents the conceptual design of a robotic rehabilitation device focused on the recovery of the elbow joint, aimed primarily at individuals who have suffered a cerebrovascular disease or trauma to that joint. The device was developed following Ullman's mechanical design methodology, which allowed the project to be structured systematically. The robot enables repetitive flexion-extension movements of the elbow, with the goal of restoring mobility to the affected upper limb.

To ensure the mechanical integrity and functional reliability of the proposed system, a structural validation was conducted through finite element analysis, along with studies for the selection and design of the electronic and instrumentation components. This development represents a step forward toward accessible, functional, and efficient rehabilitation solutions.

Keywords: Rehabilitation robot, Mechanical design, Finite element analysis, Elbow joint.

Article Info
Received May 4, 2025
Accepted Jul 1, 2025

1 Introduction

Cerebrovascular disease (CVD) encompasses a group of disorders that affect blood circulation in the brain due to obstruction, reduction, or rupture of blood vessels. These alterations can lead to neuronal damage, temporary or permanent neurological deficits, or even death. The main types of cerebrovascular disease include stroke, transient ischemic attack (TIA), cerebral venous thrombosis, cerebral vascular malformation, hypertensive encephalopathy, and vascular dementia.

When focusing on cerebrovascular disease, age is considered a risk factor. After the age of 55, the rate of experiencing this condition doubles every 10 years (Clément et al., 2018). In Mexico, as of 2021, cerebrovascular diseases were the seventh leading cause of death, with a total of 37,169 deaths, of which 19,079 were men and 18,090 were women (INEGI, 2022).

According to the Ministry of Health (Secretaría de Salud, 2021), most cases involved men over the age of 65. It is reported that one in five people who suffer a cerebral infarction dies, and three out of five are left with sequelae. Worldwide, it is the leading cause of disability in adults, which requires a much more complex rehabilitation process (Loeza, 2015).

On the other hand, according to data from the World Health Organization (WHO), traffic accidents in Mexico are the third leading cause of death and disability. It is estimated that every day, 1,700 people are hospitalized with severe injuries, and more than one hundred face disability due to the same cause. Traffic accident-related injuries are the leading cause of motor disability among young people aged 17 to 24 (CONADIS, 2020).

People who have survived this disease undergo a rehabilitation process through procedures organized within a specific program. The main goal of these treatments is to restore the patient to the highest possible level of functional capacity. In this regard, physical exercise is considered the most effective and successful rehabilitation method. Rehabilitation through physical activities allows stroke survivors to reduce their dependence on caregivers and improve their quality of life (Alrashi & Pacheco, 2019).

Robotics has emerged as a key resource, enabling effective therapies to improve patients' mobility and autonomy. This field has been widely developed and currently shows a growing application in areas related to human activity (Londoño et al., 2017). There are two main categories of rehabilitation robots: exoskeleton robots (Exo) and end-effector-based robots (EE) (Lee et al., 2020; Islam et al., 2017). Exo robots are robotic devices that attach externally to the patient's body, following the structure of the arm; while EE robots have a single point of contact with the limb, generally at the hand or forearm, and generate movements through a fixed or mobile base.

Focusing on the studies conducted on EE robots, these present different characteristics regarding mechanical structure, types of actuators, mode of operation, control techniques, as well as the type of rehabilitation they can provide to the patient (Islam et al., 2017).

In the scientific literature, a variety of robotic devices have been reported, whose function is to rehabilitate the upper limb or some of its parts. For example, (Colombo et al., 2007) and (Hu et al., 2009) present a device that allows the rehabilitation of only the wrist, while (Krebs et al., 2007) and (Takaiwa & Noritsugu, 2005) show a system for the movement of the wrist and forearm. In the same sense, (Lum et al., 2002; Lum et al., 2006) and (Tóth et al., 2005) provide a mechanism to rehabilitate the shoulder and elbow. (Amirabdollahian et al., 2007; Coote et al., 2008) and (Badesa et al., 2012; Badesa et al., 2014; Papaleo et al., 2013) show a device that produces movement of the shoulder, elbow, and forearm.

Similarly, there are robots designed to allow planar movement (Freeman et al., 2009) and axial movement (Chang et al., 2007) of the forearm; as well as the combination of axial, elevation, and yaw movements of the forearm (Reinkensmeyer et al., 2000). In the case of (Umemura, Saito, & Fujisaki, 2009), it can perform spatial movement of the shoulder and elbow. The versions of the robots by (Umemura et al., 2009) and (Liu et al., 2016) offer movement of the shoulder, elbow, forearm, and wrist, covering the largest number of joints in the arm.

In all the cases mentioned above, the different characteristics that make up the equipment are reported, such as the mechanism configuration, types of actuators, modes of operation (active or passive), control techniques, as well as the distinctive features of each model. However, the mechanical design is not presented, only the image of the robot indicating each of its joints.

In this sense, the contribution of this work is to carry out the mechanical design of a robotic system based on end-effector type parallelogram mechanisms focused on the rehabilitation of the elbow joint, capable of executing repetitive flexion and extension movements, with the aim of contributing to the recovery of functional mobility of the affected upper limb.

2 Mechanical Design Process

The proposed system was developed based on Ullman's mechanical design methodology. This approach allowed for a more structured and systematic design process. The methodology helps ensure that the product meets its objectives and requirements, optimizing functionality, cost, and efficiency (Ullman, 2010).

2.1 Product Discovery

Physical rehabilitation aims to restore patients' motor abilities through the execution of repetitive and controlled exercises. The human arm is a fundamental limb for carrying out everyday essential tasks; however, individuals who have suffered from cerebrovascular diseases or motor disabilities due to trauma may lose their autonomy. Robotics provides significant support in the recovery process for patients with these conditions.

In this context, to address the first stage of the mechanical design process, the need was identified to create a robotic device capable of generating the appropriate rehabilitation movements to assist the therapist during the patient's recovery.

2.1.1 SWOT Analysis

To identify quantifiable parameters of the robotic rehabilitation device, a SWOT analysis was conducted as follows:

Strengths:

- Infrastructure for manufacturing.
- Affordable construction cost.
- Easy to transport and operate.
- Reliability.
- Support device for patient recovery.

Opportunities:

- Sales to small and medium-sized clinics.
- Testing platform for the implementation of rehabilitation and monitoring algorithms.
- High potential for growth and expansion.
- Potential for broader implementations.

Weaknesses:

- Limited design time.
- Unattractive product image.
- Low development budget.

Threats:

- Possibility of material defects.
- Increase in raw material costs.
- Changes in product use regulations.
- Production budget overrun.

2.1.2 PRO-CON Analysis

Another alternative for assessing the feasibility of the project is by conducting a PRO-CON analysis. This approach allows for a comparative evaluation of the positive and negative aspects to determine whether the advantages outweigh the disadvantages.

As shown in Table 1, the analysis reveals a greater number of PROS compared to CONS, suggesting that the development of the project is viable and beneficial.

Table 1. Advantages and disadvantages of the robotic rehabilitation system

Advantages	Disadvantages
• Facilitates accurate arm rehabilitation.	• Requires training for use.
• Allows personalized exercises based on the patient.	• Needs maintenance to ensure proper operation.
• Reduces the need for constant therapist supervision.	• Possible resistance from patients to use technology in rehabilitation.
• Cost-effective compared to similar devices on the market.	

2.2 Product Definition

For this stage, the QFD (Quality Function Deployment) tool was used, which allows the establishment of a relationship between customer needs and the technical characteristics of the product. This tool facilitates the identification of specifications that should be prioritized by comparing them with existing products on the market. In this way, areas for improvement can be clearly visualized (Revelle et al., 1998).

To create the QFD diagram for our device, a preliminary survey was conducted with healthcare and rehabilitation professionals, aiming to complement the theoretical and technical knowledge of the development team. The QFD diagram is presented in Figure 1.

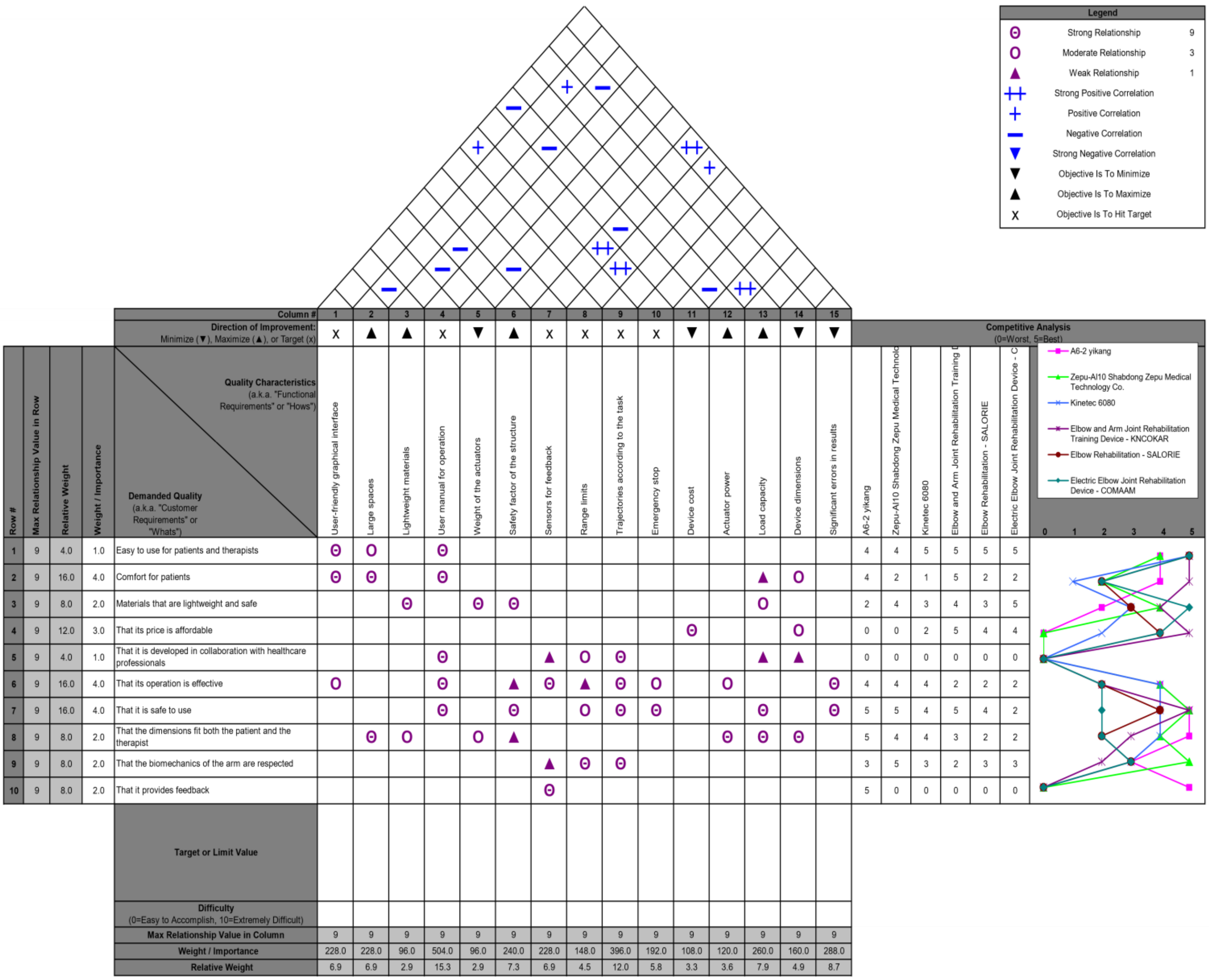

Fig. 1. QFD Diagram of the device.

2.3 Conceptual Design

The functional decomposition of the robotic rehabilitation device is carried out, starting with the definition of the general function. From this, subfunctions are identified, which subsequently allow for the generation of different concepts for each one. These concepts are evaluated to select the option that best meets all the client's needs and requirements in a comprehensive manner. The general function is shown in Figure 2.

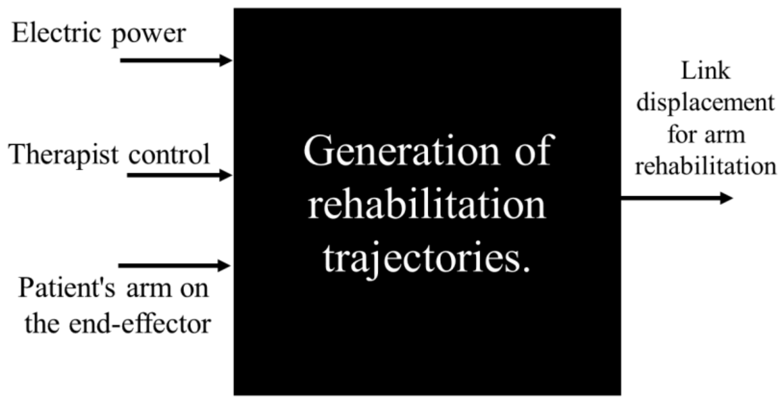

Fig. 2. General function.

After generating the general function, it is decomposed into subfunctions, which will be used to create morphological charts in order to select the best configuration for the device. It is important to mention that these subfunctions are broken down according to the convenience of the design, and the more detailed this breakdown is, the more complete the conceptual design becomes. Figure 3 shows the internal subfunctions within the general function, where the overall operation of the rehabilitation robot is further broken down.

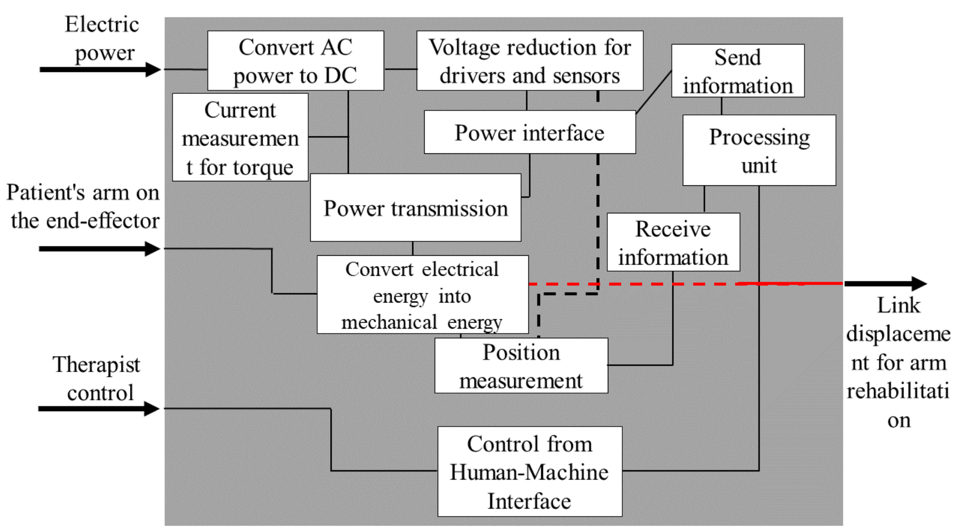

Fig. 3. Sub-functions.

To be able to break down sub-functions that result in mechanical configurations, the patient's arm at the end-effector was taken as the starting point or input. It can be observed that these sub-functions communicate internally with others, as shown in Figure 3, which leads to the displacement of the links with the purpose of rehabilitating the arm, as shown in Figure 4.

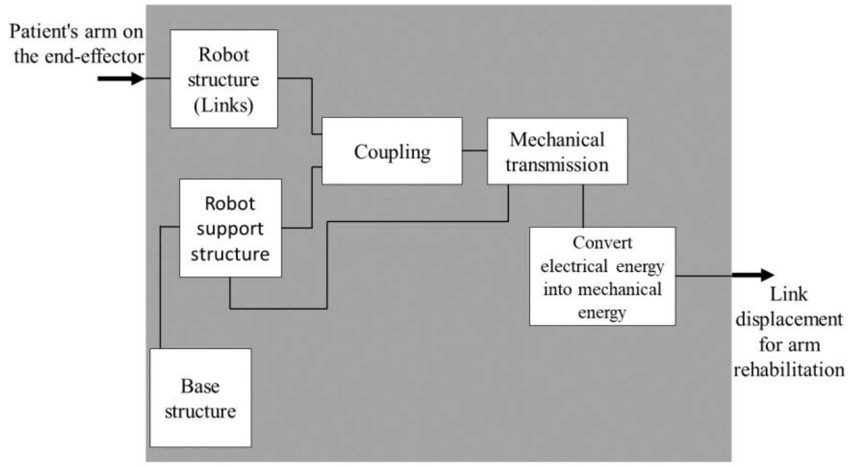

Fig. 4. Sub-functions two.

Once the sub-functions required to achieve the overall operation of the rehabilitation robot were identified, a morphological matrix was generated, as shown in Table 2. It presents the possible configurations for the instrumentation and construction of the device.

Table 2. Morphological matrix.

Subfunction	Option 1	Option 2	Option 3
Current measurement for torque	ACS712 	Shunt 	INA219 
Convert AC power to DC	AC-DC Power Supply 	Power adapter 	Industrial power supply 
Power interface	Industrial driver 	H-Bridge Module 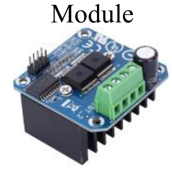	Stepper motor driver 
Convert electrical energy into mechanical energy	Industrial servomotor 	DC motor 	Stepper motor 

Position measurement	Rotary encoder 	Encoder bearing 	
Processing unit	ESP-32 	Arduino mega 	Raspberry 
Control from Human-Machine Interface	Panel with buttons 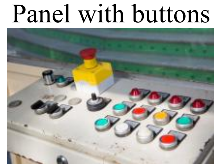	Embedded smart panel 	
Robot structure	Links made of hollow stainless steel tubing and aluminum joints.	Links made of solid aluminum with integrated machined joints.	Steel tube links with aluminum joints.
Robot support structure	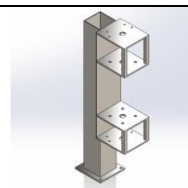	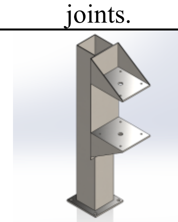	
Base structure	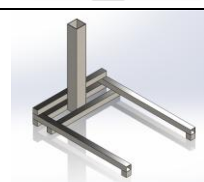	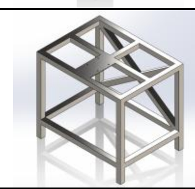	
Coupling and mechanical transmission	Transmission through aluminum shafts not directly coupled to the actuators, using bearings and flexible couplings.	Transmission through steel shafts not directly coupled to the actuators, using bearings and flexible couplings.	Direct transmission from the joint of the links to the shafts of the actuators.

After breaking down the functions and obtaining possible configurations, an evaluation of the final concepts is carried out. These are assessed based on characteristics such as cost and reliability, with the aim of selecting the most suitable concept. For this evaluation, the Pugh matrix was used, which facilitates the comparison between multiple alternatives using a *datum* defined by the designer.

It is important to consider that, when performing these evaluations, the client's requirements previously established in the QFD diagram must be taken into account. The possible conceptual design alternatives are evaluated using the values -1, 0, and +1, where +1 indicates that the concept meets the criterion better than the datum; -1 means it is inferior to the datum; and 0 indicates that both meet the criterion equally (Ullman, 2010).

Table 3 shows an example of the application of the Pugh matrix to one of the subfunctions, with the aim of illustrating the evaluation methodology that was carried out. It is important to clarify that this same procedure was applied to the other subfunctions.

Table 3. Pugh matrix.

Convert electrical energy into mechanical energy	Criteria	DC motor	Stepper motor	Industrial servomotor
Cost	15	DATUM	-1	-1
Quality	15		0	+1
Efficiency	20		0	0
Compatibility	10		0	-1
Maintenance	15		0	-1
Torque tolerance	25		-1	-1
Total	100	n/a	-40	-50

Once the evaluation of each subfunction is completed, Table 4 is obtained with the winning concepts that meet the specific needs of each one.

Table 4. Winning concepts of subfunction.

Subfunction	Concept
Current measurement for torque	Option 1 (ACS712) was selected for this application since, being a Hall effect sensor, it allows current measurement without direct contact with the power circuit. In this way, galvanic isolation is ensured, protecting the system's control electronics against possible overloads or electrical faults.
Convert AC power to DC	Option 1 (AC-DC power supply) was selected for this application because the chosen actuators have a high current consumption, and this power supply meets the demand requirements. Additionally, it features terminal blocks that allow for multiple power output connections and offers a much more affordable cost compared to the industrial power supply, without compromising the system's performance.
Power interface	Option 2 (H-Bridge Module) was selected for this application because the driver supports a current consumption of up to 43 A, with a maximum voltage of 27 V for the actuators, and it is also cost-effective.
Convert electrical energy into mechanical energy	Option 2 (DC Motor) was selected for this application because it provides a high torque of 20 Nm, which offers great tolerance for considering active rehabilitation therapy.
Position measurement	Option 1 (Rotary Encoder) was selected for this application because it offers high resolution and is mechanically adaptable to the system. Although it is not an absolute encoder, it provides great precision, and its price is more affordable compared to Option 2.
Processing unit	Option 3 (Raspberry Pi) was selected for this application because it is a low-cost computer that, unlike development boards such as the ESP32 and Arduino, offers greater processing capacity and allows the execution of multiple tasks simultaneously. In addition, the graphical interface will be implemented directly on it.
Control from Human-Machine Interface	Option 2 (Embedded smart panel) was selected for this application because it can be used on any embedded device without the need to be physically next to the machine. In addition, it is much more attractive and user-friendly for use in medical applications.
Robot structure	Option 1 was selected for this application because, being a hollow stainless-steel tube, it provides lower weight and greater strength compared to aluminum material. Additionally, both

	materials are corrosion-resistant and are ideal for use in medical machine applications.
Robot support structure	Option 1 was selected for this application because, in order to ensure a long service life of the actuators, it is necessary to include bearings and flexible couplings. This way, the stresses are not transmitted directly to the actuator shafts. This structure is adapted to accommodate such accessories as needed.
Base structure	Option 2 was selected for this application because, being a system for medical use, it is essential to consider aspects of comfort for patients, such as the height of the device and ensuring that it does not obstruct the lateral working area during rehabilitation. The table provides much greater stability to the prototype and space for instrumentation installation.
Coupling and mechanical transmission	Option 2 was selected for this application mainly because, as mentioned in the robot support structure subfunction, it is essential to preserve the actuators' lifespan. Likewise, aluminum shafts were not suitable in this case, since the forces were concentrated in that area due to the patient's weight placed on the end-effector, which caused bending. Over time, this could lead to permanent deformation in that part of the structure.

2.4 Design of the proposals in CAD

The first conceptual design is shown in the Figure 5. For this design proposal, the system was placed on a table to improve its portability; however, to prevent the robotic system from tipping over when supporting the patient's arm, two lower side supports were added. In this way, its own mechanical design becomes uncomfortable for the patient's posture during rehabilitation due to the lower side supports.

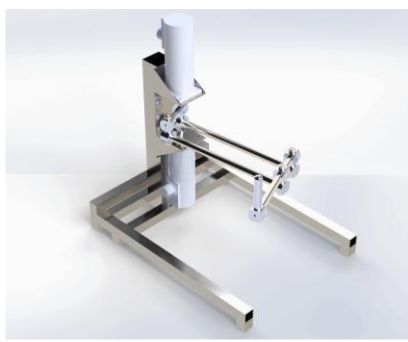

Fig. 5. Conceptual design 1.

For the second conceptual design, is shown in Figure 6, it can be observed that it already has an appropriate height for its use as a rehabilitation device. However, similar to the first conceptual design, the coupling and mechanical transmission of the actuators to the robot's links is direct; in this way, all the forces are transmitted directly to the actuators, which reduces their lifespan. Likewise, the base structure of the robot is positioned very close to the center of the table, which limits the range of motion during rehabilitation.

Fig. 6. Conceptual design 2.

Finally, the winning conceptual design is shown in Figure 7. This design is suitable in terms of height, as its construction considered that an average person in Mexico could access rehabilitation while standing, and for taller individuals, a chair with adjustable height could be used. It is also appropriate regarding the range of motion during rehabilitation. Additionally, the design considered the preservation of the actuators' lifespan by incorporating accessories that allow for traction without forcing or adding extra stress to them. Therefore, this design is considered optimal for its intended application.

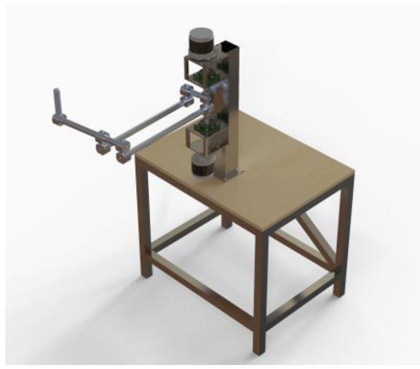

Fig. 7. Conceptual design 3.

2.5 Design of the instrumentation stage

The selected function for signal acquisition and the power stage are illustrated in Figure 8. The angular measurement of each link is carried out using optical encoders, commonly known as encoders, installed on the rear part of each motor. The connection between the encoder and the embedded system, Raspberry Pi 4, is made through an integrated circuit, the Schmitt Trigger 74LS14, in order to reduce signal noise and achieve a more accurate reading by the embedded system. Additionally, a logic level shifter circuit is used to convert signals from 5V to 3.3V.

As for the power interface (drivers), the signals coming from the Raspberry Pi 4 board pass through an optocoupler (2N25), which allows galvanic isolation of the control system, thus protecting all the electronics from possible electrical faults. Afterwards, the signals are sent to the drivers and finally to the actuators, generating direction and speed control. It is worth noting that the control electronics are powered by a DC voltage supply. For the Human-Machine Interface section, the same Raspberry Pi board is used for control. Then, the information is displayed on a screen for interaction with the therapist and the patient. The therapist will have control over the trajectories to be applied, allowing the system to be managed according to the specific needs of each patient.

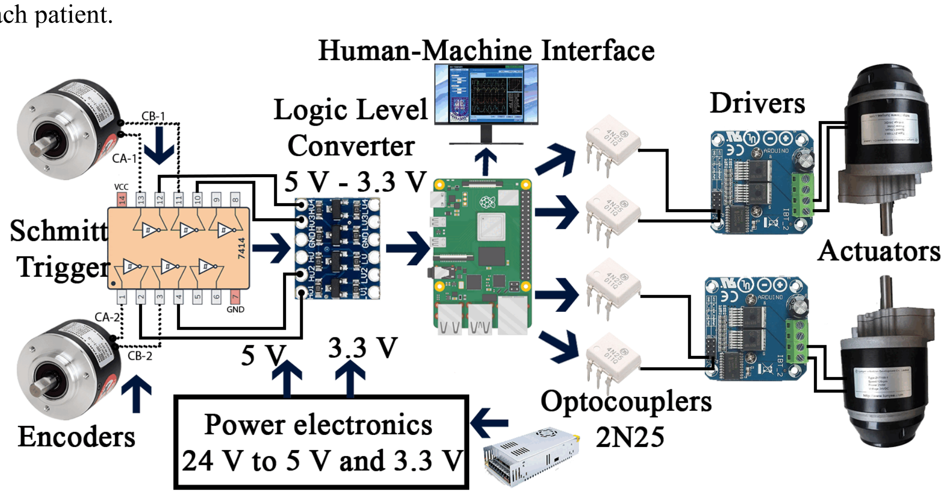

Fig. 8. Electronic circuit and graphical interface.

3 Actuator selection

To select the appropriate actuators for this application, arm strength tests were conducted using a dynamometer, evaluating flexion and extension movements in the horizontal plane. These tests were carried out on three healthy subjects with different body types, allowing the assessment of force under various physical conditions.
Table 4 presents the physical characteristics of the subjects.

Table 4. General data of the subjects in the strength tests

Subjects	Age (years)	Height (m)	Weight (kg)
1	22	1.76	70
2	21	1.62	73
3	22	1.81	98

Once the characteristics of the subjects were defined prior to the tests, and after performing a series of repetitions, the force results shown in Table 5 were obtained.

Table 5. Results of strength tests

Subjects	No. of tests	Average force (N)
1	4	62.7
2	4	46.4
3	4	88.4

The movement performed by the subjects during the tests corresponds to the motion executed during elbow rehabilitation. The selected force value was 88.4 N, considering that this represents an excess force, in order to provide a sufficient margin for active therapy applications. To obtain the torque data, the robotic formula that relates the forces applied at the end-effector **(F)** with the transposed Jacobian was used, as shown in Equation 1 (Craig, 2009).

$$\tau = J^T(q)F \,, \tag{1}$$

where τ is the vector of joint torques, $J(q)^T$ is the transposed Jacobian matrix that relates joint movements to the forces at the end-effector, and F is the vector of forces applied at the end-effector. The obtained torques are shown in Figure 9.

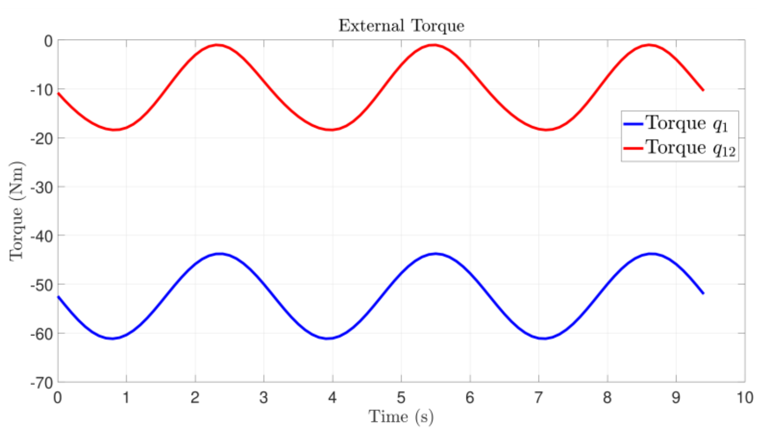

Fig. 9. Torque graph obtained.

On the other hand, the work of (Krebs et al., 2004) established that during elbow extension in individuals with upper limb weakness, a force of 28 N is typically generated. Considering an average moment arm of 0.3 m, the resulting torque is 8.4 Nm. Based on this data, in the obtained torque graph, where the maximum torque of the q_{12} joint was considered to be 20 Nm, and considering the actuators available on the market, it was decided to use a 20 Nm actuator. In this way, a tolerance range greater than twice the requirement for a person with weakness is achieved, allowing for treatments focused on the generation or recovery of strength in the limb.

4 Finite element analysis

When structurally analyzing systems, it often involves highly complex differential equations that, in most cases, do not have an analytical solution. Faced with this difficulty, the Finite Element Method (FEM) proves to be a very helpful tool.

The fundamental principle of FEM consists of discretizing the system's structure, dividing it into a set of finite elements connected to each other through nodes. In this way, the problem is transformed into a system of algebraic equations, which allows it to be solved in a less complex manner.

The process begins by analyzing each element independently. Then, a structural assembly is performed by considering equilibrium conditions and displacement compatibility at the nodes. Finally, the solution of the system is obtained, which results in the nodal displacements, and from these, the global behavior of the structure can be analyzed (Vásquez & López, 2001; Fitzgerald, 1996).

To ensure the integrity of the entire mechanical structure, stress analyses were carried out using SolidWorks software. The base structure and the part that supports the robot were designed using AISI-1020 steel. Regarding the links, these are composed of two materials: stainless steel hollow tube (AISI-304) and 1060 aluminum for the joints.

In the analysis of the links, the average mass of a human arm was considered to be 3.25 kg, which corresponds to an applied force of 31.8825 N.

Analysis of link one

Figure 10 shows the Von Mises stress distribution for the first link. It can be observed that the region with the highest stress is located in the stainless steel tube, near the area of fixed geometries.

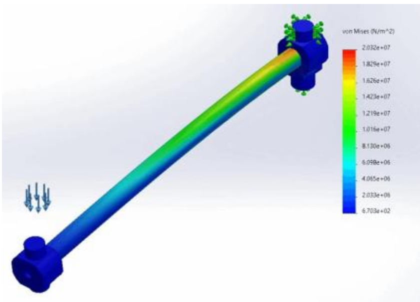

Fig. 10. Von Mises stress of link 1.

On the other hand, Figure 11 shows the nodal displacements, with a maximum value of 7.647×10^{-1} mm. In addition, the safety factor was calculated, yielding a value of 3.586, which indicates that the structure can adequately withstand the applied stresses in that area, without risk of structural failure.

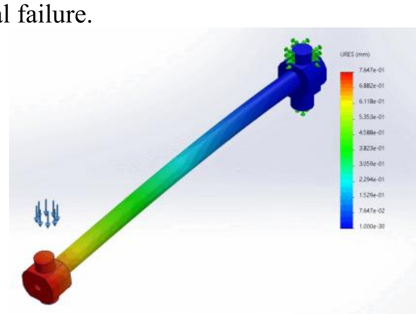

Fig. 11. Nodal displacements of link 1.

Analysis of link two

Figure 12 shows the Von Mises stress distribution of the second link. It can be observed that the region with the highest stress is located in the stainless steel tube, near the area with fixed geometries.

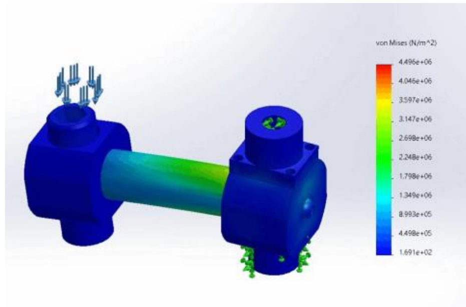

Fig. 12. Von Mises stress of link 2.

Similarly, Figure 13 illustrates the nodal displacements, where a maximum value of 1.332×10^{-2} mm was identified. In this case, the calculated safety factor was 14.915, which indicates that the structure has a high capacity to withstand the applied loads without risk of failure.

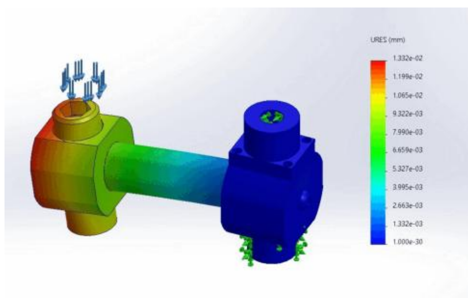

Fig. 13. Nodal displacements of link 2.

Analysis of link three

In Figure 14, the Von Mises stress distribution of the third link is shown. It can be observed that the region with the highest stress is located in the stainless steel tube, near the area with fixed geometries.

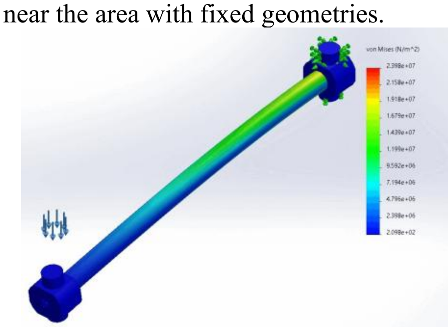

Fig. 14. Von Mises stress of link 3.

On the other hand, Figure 15 displays the nodal displacements, where a maximum displacement of 7.258×10^{-1} mm was identified. Additionally, a safety factor of 3.7 was calculated, indicating that the structure can withstand the applied loads without risk.

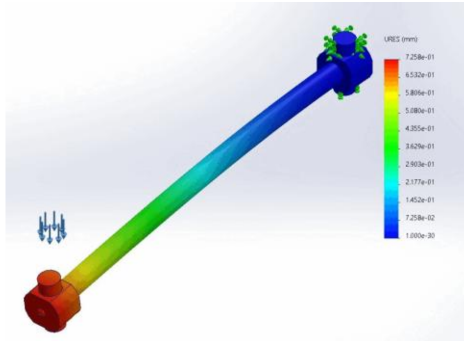

Fig. 15. Nodal displacements of link 3.

Analysis of link four

In Figure 16, the Von Mises stress distribution of the link four assembly is shown. It can be observed that the region with the highest stress is located in the stainless steel tube, near the second area of fixed geometries.

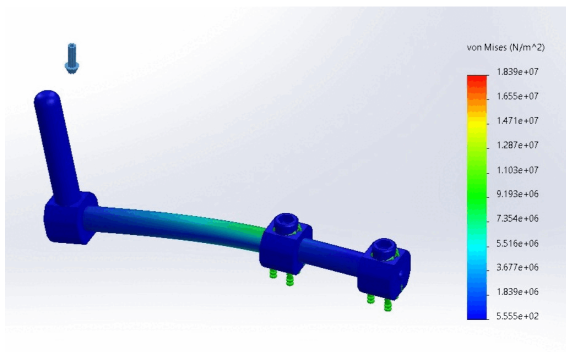

Fig. 16. Von Mises stress of link 4.

On the other hand, Figure 17 illustrates the nodal displacements obtained in the analysis, where the maximum displacement was 1.046×10^{-1} mm. In addition, a safety factor of 4.8 was obtained, which ensures that the structure is capable of withstanding the load conditions without compromising its integrity.

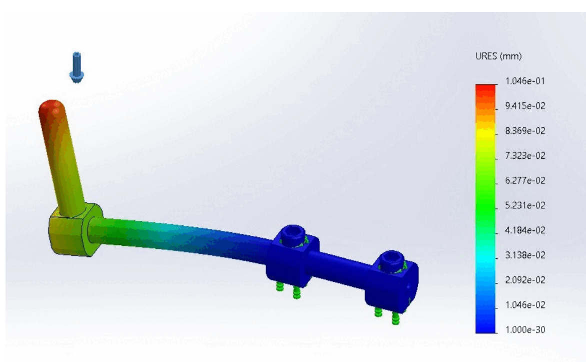

Fig. 17. Nodal displacements of link 4

Analysis of robot support structure

Regarding the robot support structure, two forces are considered and applied to four plates. For the lateral plates, the mass of the motors, screws, and encoders is taken into account, resulting in a total of 3.999076 kg, which corresponds to an applied force of 39.2248 N on each plate.

On the other hand, the internal plates consider the masses of the bearings, screws, assembled links, the human arm, and flexible couplings, resulting in a total of 4.80864 kg per plate. Therefore, a force of 47.1728 N is applied to each internal plate.

Figure 18 shows the Von Mises stress distribution of the robot support structure. It can be observed that the regions with the highest stress are located on the lateral and internal plates.

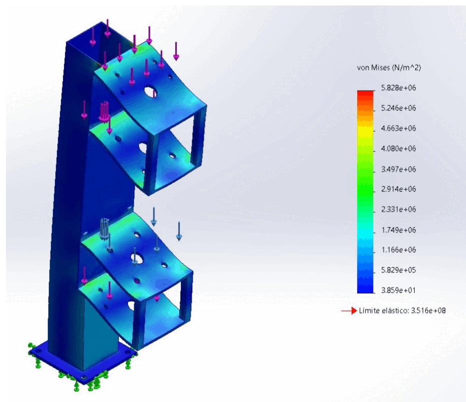

Fig. 18. Von Mises stress of the robot support structure.

Regarding the nodal displacements, Figure 19 shows that the maximum displacement value is 3.063×10^{-2} mm. Additionally, the analysis yielded a safety factor of 60.321, confirming that the structure operates with a wide margin against potential failure.

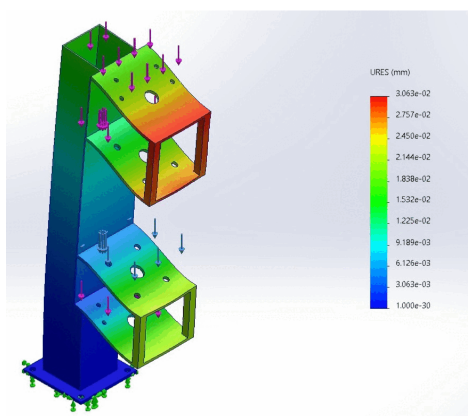

Fig. 19. Nodal displacements of the robot support structure.

Analysis of base structure

In the base structure, the masses of the robot support structure, its accessories, the assembled links, and the human arm were considered, and therefore a force of 245.02 N was applied on the upper surface.

Figure 20 shows the Von Mises stress distribution of the base structure. It can be observed that the region with the highest stress is located in the attachment area of the robot support structure and the upper steel tubes (PTRS).

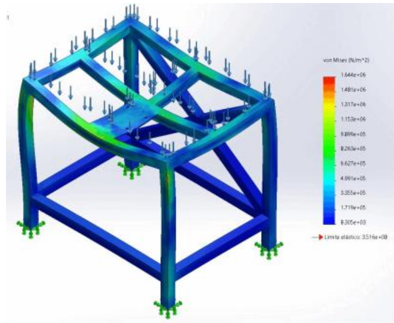

Fig. 20. Von Mises stress of the base structure.

Figure 21 displays the nodal displacements obtained for the base, highlighting a maximum displacement value of 1.452×10^{-2} mm. Additionally, a safety factor of 213.813 was obtained, which guarantees adequate structural strength with no indication of failure, and can even be considered an extremely large safety margin.

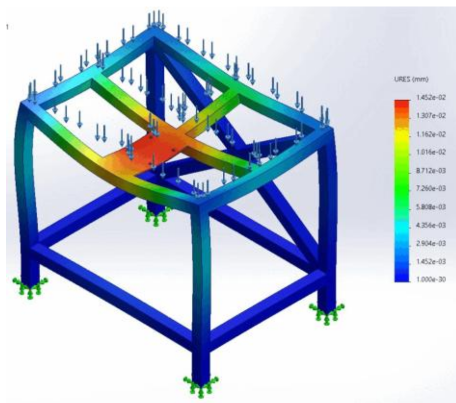

Fig. 21. Nodal displacements of the base structure.

5 Conclusions

The contribution of this work focuses on the design of a robotic system using the Ullman methodology, resulting in the following outcomes:

The methodology provided insights into the relevance of developing the project, the users' needs for operating the device, and the essential requirements to meet those needs. This process led to the definition of system functions and subfunctions, which guided the selection of the mechanical structure and the electronic and electrical components during the conceptual design phase, using a morphological table and a PUGH matrix.

A systematic procedure regarding was presented for selecting of the motor torque based on experimental measurements of the force generated by healthy individuals and data reported in the literature the strength of individuals with upper limb weakness. The result was a minimum motor torque of 20 Nm.

It was demonstrated that the robot's structure and mechanism can support the weight of an arm, whether from a healthy or disability person, without compromising patient safety due to mechanical failure from excessive stress. This was validated through Von Mises stress analysis across each of the links and supports of the mechanism, resulting in a minimum safety factor of 3.586, and a maximum displacement of 7.64×10^{-1} mm.

6 Acknowledgments

The first author, Elihu H. Ramirez-Dominguez, would like to thank the Secretaría de Ciencia, Humanidades, Tecnología e Innovación (SECIHTI) for the scholarship awarded to CVU 1316798.

References

Alrashi, M., & Rodríguez Pacheco, S. (2019). El accidente cerebrovascular y su tratamiento fisioterapéutico. *Ciencia & Conciencia, 2*(1).

Amirabdollahian, F., Loureiro, R., Gradwell, E., Collin, C., Harwin, W., & Johnson, G. (2007). Multivariate analysis of the Fugl-Meyer outcome measures assessing the effectiveness of GENTLE/S robot-mediated stroke therapy. *Journal of NeuroEngineering and Rehabilitation, 4*(1), 4. https://doi.org/10.1186/1743-0003-4-4

Badesa, F. J., Morales, R., Garcia-Aracil, N., Sabater, J. M., & Perez-Vidal, C. (2012). Multimodal interfaces to improve therapeutic outcomes in robot-assisted rehabilitation. IEEE Transactions on Systems, Man, and Cybernetics - Part C: Applications and Reviews, 42(6), pp. 1152–1158. https://doi.org/10.1007/978-3-319-03838-4_16

Badesa, F. J., Morales, R., Garcia-Aracil, N., Sabater, J. M., Casals, A., & Perez-Vidal, C. (2014). Auto-adaptive robot-aided therapy using machine learning techniques. *Computer Methods and Programs in Biomedicine, 116*(2), pp. 123–130. https://doi.org/ 10.1016/j.cmpb.2013.09.011

Chang, J. J., Tung, W. L., Wu, W. L., Huang, M. H., & Su, F. C. (2007). Effects of robot-aided bilateral force-induced isokinetic arm training combined with conventional rehabilitation on arm motor function in patients with chronic stroke. *Archives of Physical Medicine and Rehabilitation, 88*(10), pp. 1332–1338. https://doi.org/10.1016/j.apmr.2007.07.016

Clément, M. E., Romano, L. M., Furnari, A., Abrahín, J. M., Marquez, F., Coffey, P., Rodriguez, L., Carabajal, V., Gonorazk, S., & Ioli, P. (2018). Incidencia de enfermedad cerebrovascular en adultos: estudio epidemiológico prospectivo basado en población cautiva en Argentina. *Neurología Argentina, 10*(1), pp. 8–15. Elsevier. https://doi.org/10.1016/j.neuarg.2017.09.002

Coote, S., Murphy, B., Harwin, W., & Stokes, E. (2008). The effect of the GENTLE/s robot-mediated therapy system on arm function after stroke. *Clinical Rehabilitation, 22*(5), pp. 395–405. https://doi.org/10.1177/0269215507085060

Colombo, R., Pisano, F., Mazzone, A., Delconte, C., Micera, S., & Carrozza, M. C. (2007). Design strategies to improve patient motivation during robot-aided rehabilitation. *Journal of NeuroEngineering and Rehabilitation, 4*(1), 3. https://doi.org/10.1186/1743-0003-4-3

Freeman, C. T., Hughes, A. M., Burridge, J. H., Chappell, P. H., Lewin, P. L., & Rogers, E. (2009). A robotic workstation for stroke rehabilitation of the upper extremity using FES. *Medical Engineering & Physics, 31*(4), pp. 364–373. https://doi.org/10.1016/j.medengphy.2008.05.008

Consejo Nacional para el Desarrollo y la Inclusión de las Personas con Discapacidad (CONADIS). (2020). *Los accidentes de tránsito y la discapacidad*. Gobierno de México. https://www.gob.mx/conadis/articulos/los-accidentes-de-transito-y-la-discapacidad (Consultado el 22 de marzo de 2025)

Craig, J. J. (2009). Introduction to robotics: Mechanics and control (3rd ed.). Pearson Education. ISBN 978-81-317-1836-0

Fitzgerald, R. W. (1996). *Mecánica de materiales* (2ª ed.). Alfaomega Grupo Editor. ISBN 970-15-0154-3

Instituto Nacional de Estadística y Geografía (INEGI). (2022). *Estadísticas de defunciones registradas 2021. Nota técnica*. Aguascalientes, México. https://www.inegi.org.mx/contenidos/programas/mortalidad/doc/nota_tecnica_2021.pdf (Versión electrónica, consultada en abril de 2025)

Islam, M. R., Spiewak, C., Rahman, M. H., & Fareh, R. (2017). A brief review on robotic exoskeletons for upper extremity rehabilitation to find the gap between research prototype and commercial type. *Advances in Robotics & Automation, 6*(2), pp. 10–4172. https://doi.org/10.4172/2168-9695.1000177

Lum, P. S., Burgar, C. G., Shor, P. C., Majmundar, M., & Van der Loos, M. (2002). Robot-assisted movement training compared with conventional therapy techniques for the rehabilitation of upper-limb motor function after stroke. *Archives of Physical Medicine and Rehabilitation, 83*(7), pp. 952–959. https://doi.org/10.1053/apmr.2001.33101

Lum, P. S., Burgar, C. G., Van der Loos, H. F. M., Shor, P. C., Majmundar, M., & Yap, R. (2006). MIME robotic device for upper-limb neurorehabilitation in subacute stroke subjects: A follow-up study. *Journal of Rehabilitation Research and Development, 43*(5), pp. 631–642. https://doi.org/10.1682/jrrd.2005.02.0044

Krebs, H. I., Ferraro, M., Buerger, S. P., Newbery, M. J., Makiyama, A., Sandmann, M., Lynch, D., Volpe, B. T., & Hogan, N. (2004). Rehabilitation robotics: Pilot trial of a spatial extension for MIT-Manus. *Journal of NeuroEngineering and Rehabilitation*, pp. 1–15. https://doi.org/10.1186/1743-0003-1-5

Krebs, H. I., Volpe, B. T., Williams, D., Celestino, J., Charles, S. K., Lynch, D., & Hogan, N. (2007). Robot-aided neurorehabilitation: A robot for wrist rehabilitation. *IEEE Transactions on Neural Systems and Rehabilitation Engineering, 15*(3), pp. 327–335. https://doi.org/10.1109/TNSRE.2007.903899

Lee, S. H., Park, G., Cho, D. Y., Kim, H. Y., Lee, J.-Y., Kim, S., Park, S.-B., & Shin, J.-H. (2020). Comparisons between end-effector and exoskeleton rehabilitation robots regarding upper extremity function among chronic stroke patients with moderate-to-severe upper limb impairment. *Scientific Reports, 10*(1), 1806. https://doi.org/10.1038/s41598-020-58630-2

Liu, L., Shi, Y. Y., & Xie, L. (2016). A novel multi-DOF exoskeleton robot for upper limb rehabilitation. *Journal of Mechanics in Medicine and Biology, 16*(6), 1640023. https://doi.org/10.1142/S0219519416400236

Umemura, A., Saito, Y., & Fujisaki, K. (2009). A study on power-assisted rehabilitation robot arms operated by patient with upper limb disabilities. In *Proceedings of the IEEE International Conference on Rehabilitation Robotics (ICORR)* (pp. 451–456). IEEE.

Rosati, G., Gallina, P., & Masiero, S. (2007). Design, implementation and clinical tests of a wire-based robot for neurorehabilitation. *IEEE Transactions on Neural Systems and Rehabilitation Engineering*, 15(4), 560–569. https://doi.org/10.1109/TNSRE.2007.908560

Loeza, M. P. (2015). Introducción a la rehabilitación robótica para el tratamiento de la enfermedad vascular cerebral: revisión. *Revista Mexicana de Medicina Física y Rehabilitación, 27*(2), pp. 44–48.

Londoño, J. A. A., Caicedo Bravo, E., & Castillo García, J. F. (2017). Aplicación de tecnologías de rehabilitación robótica en niños con lesión del miembro superior. *Revista de la Universidad Industrial de Santander. Salud, 49*(1), pp. 103–114. http://dx.doi.org/10.18273/revsal.v49n1-2017010

Papaleo, E., Zollo, L., Spedaliere, L., & Guglielmelli, E. (2013). Patient-tailored adaptive robotic system for upper-limb rehabilitation. In *2013 IEEE International Conference on Robotics and Automation (ICRA)* (pp. 3860–3865). IEEE. https://doi.org/ 10.1109/ICRA.2013.6631120

Reinkensmeyer, D. J., Kahn, L. E., Averbuch, M., McKenna-Cole, A., Schmit, B. D., & Rymer, W. Z. (2000). Understanding and treating arm movement impairment after chronic brain injury: Progress with the ARM guide. *Journal of Rehabilitation Research and Development, 37*(6), pp. 653–662.

Revelle, J. B., Moran, J. W., & Cox, C. A. (1998). *The QFD handbook*. John Wiley & Sons.

Secretaría de Salud. (2021, octubre 29). *En 2021, ictus o enfermedad vascular cerebral ocasionó más de 37 mil decesos en México* [Comunicado de prensa]. Gobierno de México. https://www.gob.mx/salud/prensa/531-en2021-ictus-o-enfermedad-vascular-cerebral-ocasiono-mas-de-37-mil-decesos-en-mexico?utm_source=chatgpt.com

Takaiwa, M., & Noritsugu, T. (2005). Development of wrist rehabilitation equipment using pneumatic parallel manipulator. In *Proceedings of the IEEE International Conference on Robotics and Automation (ICRA)* (pp. 2302–2307). IEEE. https://doi.org/10.1109/ROBOT.2005.1570481

Tóth, A., Fazekas, G., Arz, G., Jurak, M., & Horváth, M. (2005). Passive robotic movement therapy of the spastic hemiparetic arm with REHAROB: Report of the first clinical test and the follow-up system improvement. In *Proceedings of the 9th International Conference on Rehabilitation Robotics (ICORR)* (pp. 127–130). IEEE. https://doi.org/10.1109/ICORR.2005.1501067

Ullman, D. G. (2010). *The Mechanical Design Process* (4th ed.). McGraw-Hill. ISBN 978-0-07-297574-1

Vásquez, M., & López, E. (2001). El método de los elementos finitos aplicado al análisis estructural. España: Editora Noela. ISBN: 84-8801206-3